Macromolecular Research, Vol. 14, No. 6, pp 610-616 (2006)

# Styrenic Polymer/Organoclay Nanocomposite Prepared via *in-situ* Polymerization with an Azoinitiator Linked to an Epoxy Oligomer

**Han Mo Jeong*, Mi Yeon Choi, Min Seok Kim, Jin Hee An, Jin Su Jung, and Jae Hoon Kim**

*Department of Chemistry, University of Ulsan, Ulsan 680-749, Korea*

**Byung Kyu Kim and Sung Man Cho**

*Department of Polymer Science and Engineering, Pusan National University, Busan 609-735, Korea*

*Received July 20, 2006; Revised October 9, 2006*

**Abstract:** An azoinitiator linked to an epoxy oligomer, which could easily diffuse into the organoclay gallery and swell it, was used as an initiator to enhance the delamination of an organoclay, Cloisite 25A, in a matrix of styrenic polymers, poly(styrene-*co*-acrylonitrile) and polystyrene, during the preparation of a nanocomposite via an *in-situ* polymerization method. X-ray diffraction results and transmission electron microscopic observation of the morphology showed that the epoxy segment enhanced not only the delamination but also the extrication of ammonium cations from the organoclay gallery into the polymer matrix. The latter phenomenon induced the structural change of the alkyl group of ammonium cations in the gallery from a bilayer to monolayer structure, and also decreased the glass-rubber transition temperature as measured by a differential scanning calorimeter and dynamic mechanical analyzer.

*Keywords*: styrenic polymers, organoclay, epoxy oligomer, nanocomposite.

## Introduction

The field of polymer-layered silicate nanocomposites has attracted considerable attention over the past decade because they often exhibit substantially enhanced properties compared to pristine polymers or conventional composites, even when prepared with a very small amount of layered silicate.[1-8] The improved properties of these nanocomposites include mechanical, thermal, barrier, and flame-retardant properties. Because the unique properties of the nanocomposites arise from the maximized interfacial contact between the organic and inorganic phases, fillers with a high surface-to-volume ratio are commonly used. Layered silicates such as montmorillonite, which are composed of stacks of 1 nm thick parallel lamellae with a high aspect ratio, are typical fillers.

Two ideal morphologies of polymer-layered silicate nanocomposites are intercalated and exfoliated structures. The intercalated structure is a self-assembled, well-ordered, and multilayered structure in which the extended polymer chains are inserted into the gallery space between parallel individual silicate layers. In the exfoliated structure, the individual silicate layers are delaminated and randomly dispersed in the polymer matrix separately. However, many nanocomposites have morphologies of both intercalated and exfoliated structures, together with partially exfoliated structures, where small stacks of silicate layers are dispersed in the polymer matrix.[9,10]

Because exfoliated nanocomposites usually provide the best property enhancements due to a large interfacial area and homogeneous dispersion, many efforts have been devoted to the design of methods that improve the delamination of silicate layers in the polymer matrix.[9,11,12] Because there is an entropy loss in order for the polymer chain to diffuse into the gallery, the methods which induce sufficiently favorable enthalpic interactions between the polymer and layered silicate are necessary to obtain the nanocomposites.[13]

Hydrophilic polymers, such as poly(ethylene oxide) or poly(vinyl alcohol), for example, can diffuse into the gallery of sodium montmorillonite (Na-MMT) to yield nanocomposites, because the gallery of Na-MMT is hydrophilic in nature, where the excess negative charge on the surface of silicate layers is balanced by the $Na^+$ cations that exist between the silicate layers.[14,15] The diffusion of hydrophobic polymers into the gallery of hydrophilic Na-MMT, however, is strictly limited. This difficulty can be overcome when the interlayer cation, $Na^+$, is replaced with organic cations such as ammonium ions with long alkyl chains to yield organoclay. This organoclay has a low surface polarity and enhanced affinity with hydrophobic matrix polymers to create nano-

*Corresponding Author. E-mail: hmjeong@mail.ulsan.ac.kr

composites.

Block or graft copolymers containing a block which is identical or miscible with the matrix polymer, and another block which has an affirmative enthalpic interaction with the layered silicate, can be effectively utilized in the preparation of nanocomposites.[16] For example, a block copolymer of polyethylene and poly(ethylene glycol) (PEG) can be utilized in the preparation of a polyethylene/Na-MMT nanocomposite,[17] and a block copolymer of polypropylene (PP) and poly(methyl methacrylate) (PMMA) can be utilized for a PP/organoclay nanocomposite.[13]

We reported that the dispersion of Na-MMT in the PMMA matrix was enhanced when PMMA/Na-MMT nanocomposites were prepared via an *in-situ* polymerization with a macroazoiniator (MAI), a condensation polymer of 4,4'-azobis (4-cyanopentanoic acid) (ACPA) and a PEG diol (molecular weight 2,000) with the structure shown as Chemical Structure 1.[18] These results showed that the PEG segment linked to the matrix polymer could enhance the dispersion of Na-MMT, because PEG has a strong affinity toward Na-MMT. A similar result was observed in the polyacrylonitrile/Na-MMT nanocomposites prepared via an *in-situ* polymerization with the same MAI.[19]

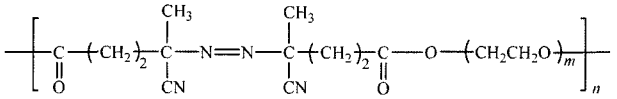

Chemical Structure 1

We also observed that the dispersion of the organoclay in the polystyrene (PS) matrix was enhanced when another MAI, the condensation polymer of ACPA and $\alpha$, $\omega$-bis(3-aminopropyl) poly(dimethyl siloxane) (PDMS) (molecular weight 5,000: Chemical Structure 2), was used in the preparation of the PS/organoclay nanocomposite via an *in-situ* polymerization, because there exists affirmative interactions between the organoclay and the PDMS segment linked to PS.[20]

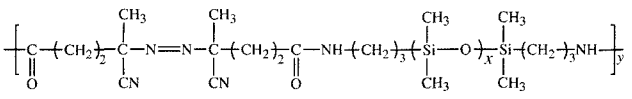

Chemical Structure 2

When preparing nanocomposites by the melt compounding method, a small amount of swelling agent, which can easily diffuse into the gallery and expand the gallery height, can improve exfoliation. Kato *et al.* utilized a polyolefin oligomer with a telechelic OH group in the preparation of the PP/organoclay nanocomposite,[21-23] and Ishida *et al.* reported that the epoxy oilgomer (Chemical Structure 3) was effective as a swelling agent in the melt compounding of organoclays with many kinds of polymers.[24]

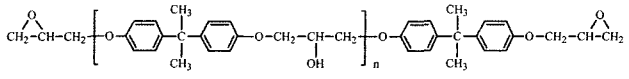

Chemical Structure 3

In the present study, we linked an azoinitiator, ACPA, to the above epoxy oligomer by an esterification reaction and utilized it as an initiator in the preparation of organoclay nanocomposites of styrenic polymers, PS, and poly(styrene-*co*-acrylonitrile) (SAN) via an *in-situ* polymerization method, because we anticipated that the initiator could easily diffuse into the gallery and cause inter-gallery radical polymerization inducing exfoliation. The morphological, thermal, and mechanical properties of these nanocomposites were examined and compared to those prepared in the absence of an epoxy oligomer.

## Experimental

**Materials.** The epoxy oligomer of Chemical Structure 3, was purchased from Aldrich, and used as received. The molecular weight was 1,075, which means that the average value of $n$ in Chemical Structure 3 is 2.6. Styrene (BASF Korea), acrylonitrile (AN, Aldrich), 2,2'-azobisisobutyronitrile (AIBN, Junsei Chemical), 4,4'-azobis(4-cyanopentanoic acid) (ACPA, Fluka), thionyl chloride ($SOCl_2$, Duksan Pharmaceutical), triethylamine (Duksan Pharmaceutical), methanol (Aldrich), tetrahydrofuran (THF, Aldrich), dimethylformamide (DMF, Adrich) and methylene chloride (Aldrich) were used as received. An organoclay, Cloisite 25A, was purchased from Southern Clay Products Inc. It was reported that the cations of natural montmorillonite in this organoclay were replaced by dimethyl, hydrogenated tallow, and 2-ethylhexyl quaternary ammonium ions. The organoclay's modifier concentration is 95 meq/100 g-clay and the weight loss on ignition is 34%.

**Preparation of ACPA Linked to Epoxy Oligomer.** 4,4'-Azobiscyanpentanoyl chloride (ACPC) was prepared by the reaction of ACPA and thionyl chloride, according to a method described previously.[25] The ACPC was reacted with the epoxy oligomer to link the -CO-Cl group of ACPC and -OH group of epoxy oligomer by an esterification reaction. Specifically, in the 250 mL of THF maintained at 0~5 °C, 10 mmol of epoxy oligomer, 26 mmol of ACPC, and 32 mmol of triethylamine were dissolved. The mixture was continuously stirred for 24 h at 0~5 °C to complete the esterification reaction. After evaporation of THF at 25 °C under vacuum, the reaction mixture was washed three times with a methanol/distilled water mixture (1/4 by volume) to remove triethylamine-HCl salt. It was dried for 12 h at 25 °C under vacuum. The yield by weight was about 65%. The azo group concentration was calculated through the $^1$H-NMR spectrum by comparing the peak area of the aromatic protons at 6.0~

8.0 ppm and aliphatic protons at 1.4~1.7 ppm, and was found to be 1.61 mmol/g.

**Preparation of Nanocomposites.** The styrenic polymer/organoclay nanocomposites were prepared by *in situ* polymerization of the styrene or styrene/acrylonitrile mixture (75/25 by weight) in the presence of organoclay at 60 °C with constant stirring by a magnetic bar under a $N_2$ atmosphere for 24 h. The epoxy oligomer linked to ACPA (ACPC-Epoxy) or AIBN was used as an azoinitiator and the recipes are shown in Table I. The prepared styrenic polymer/organoclay nanocomposites were crushed into a powder and dried at 80 °C for 48 h under vacuum to remove low molecular weight components.

**Measurements.** The number-average molecular weight ($\overline{M}_n$) and weight-average molecular weight ($\overline{M}_w$) were evaluated at 43 °C with gel permeation chromatography (GPC, Waters M510). The nanocomoposite was dissolved in DMF and organoclay was removed by centrifugation prior to measurement.

X-ray diffraction (XRD) patterns were obtained with an X-ray diffractometer (X'PERT, Philips) using $CuK_\alpha$ radiation ($\lambda$=1.54 Å) as the X-ray source. The diffraction angle was scanned from 1.2 ° at a rate of 1.2 °/min.

The morphology of the nanocomposites was examined with a transmission electron microscope (TEM, Hitachi H-8100) with an accelerating voltage of 200 kV. The samples for TEM observation were first prepared by putting a nanocomposite powder/epoxy resin mixture into a capsule and curing the epoxy resin at 25 °C for 24 h in a vacuum oven. The cured epoxy resin, which contained a nanocomposite, was then microtomed by a diamond knife into 80 nm thick slices.

Dynamic mechanical properties were measured using a dynamic mechanical thermal analyzer (Rheometry Scientific DMTA MK III), with a bending mode at a heating rate of 5 °C/min and 1 Hz.

Differential scanning calorimetry (DSC) was carried out with a DSC-2910 (TA Instrument) at a heating and cooling rate of 10 °C/min, with 7.5 mg of sample. The sample remained at 180 °C for 5 min in the DSC, and was then cooled down to 25 °C. The glass transition temperature ($T_g$) was determined in a subsequent heating scan.

## Results and Discussion

**XRD.** In a nanocomposite with an intercalated structure, multilayered features with alternating polymer-silicate layers are usually retained, so an increased d-spacing between the silicate layers can be detected by XRD. However the exfoliated structure no longer gives a coherent wide angle ($2\theta > 1°$) XRD signal, because the distances between the silicate layers are expanded far apart and the layers are sufficiently disordered.[9,10]

In order to monitor the swelling of the epoxy oligomer in the absence of a polymer matrix, the organoclay/epoxy oligomer nanocomposites (10/2, 10/10 by weight) were prepared by evaporating $CH_2Cl_2$ after dispersing the mixture in $CH_2Cl_2$ for 24 h at 25 °C. The XRD patterns of these nanocomposites are shown in Figure 1 together with that of pristine organoclay, where we can see that the organoclay has a peak at $2\theta$=4.7 °, and two organoclay/epoxy oligomers have peaks at $2\theta$=3.1 ° and at $2\theta$=2.9 °, respectively. This shows that the gallery height calculated by Bragg's law, $d=\lambda/2\sin\theta$, increased from 18.8 to 28.5 Å and 30.2 Å by the intercalation of the epoxy oligomer into the gallery of organoclay; however, the degree of swelling is not so dependent on the amount of epoxy oligomer.

Alkyl chains of ammonium ions can have various orientations and arrangements in the gallery, which are dependent on the packing density, temperature, chain length, and charge density of the clay.[1,26,27] They can have lateral monolayer, lateral bilayer, or a pseudo-trimolecular layer structure and the gallery height is dependent on this structure. A simple calculation of the gallery height of the organoclay suggests that $d_{trilayer}=9.6+3\times4.6=23.4$(Å) (corresponding to $2\theta \fallingdotseq$

**Table I. Recipe for the Preparation of the Styrenic Polymer/Organoclay Nanocomposites**

| Designation | Monomer | | Initiator | | | Organoclay |
|---|---|---|---|---|---|---|
| | Styrene (g) | Acrylonitrile (g) | AIBN (g) | ACPC-Epoxy (g) | Amount of Azo Group (mmol) | |
| SAN Nanocomposite | | | | | | |
| NEP0 | 75 | 25 | 0.50 | - | 0.30 | 5 |
| NEP1 | 75 | 25 | - | 1.67 | 0.27 | 5 |
| NEP3 | 75 | 25 | - | 5.01 | 0.81 | 5 |
| NEP5 | 75 | 25 | - | 8.34 | 1.34 | 5 |
| PS Nanocomposite | | | | | | |
| SEP0 | 100 | - | 0.50 | - | 0.30 | 5 |
| SEP1 | 100 | - | - | 1.67 | 0.27 | 5 |
| SEP3 | 100 | - | - | 5.01 | 0.81 | 5 |
| SEP5 | 100 | - | - | 8.34 | 1.34 | 5 |

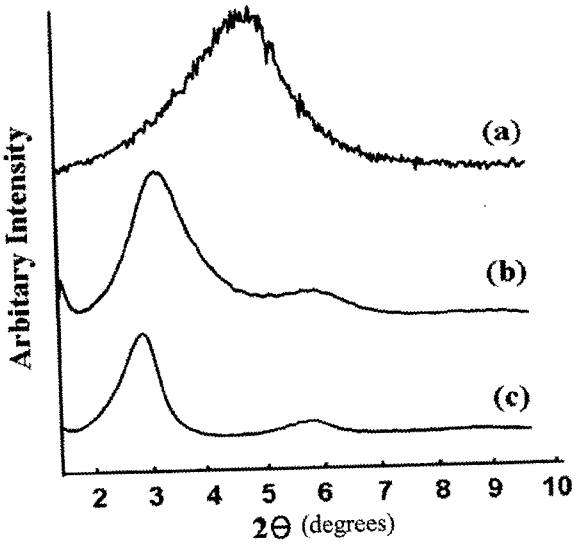


**Figure 1.** XRD patterns of (a) Cloisite 25A, and Cloisite 25A/epoxy oligomer nanocomposites ((b) 10/2 and (c) 10/10 by weight).

3.8°), $d_{bilayer}=9.6+2\times4.6=18.8$(Å) (corresponding to $2\theta \fallingdotseq 4.7°$), and $d_{monolayer}=9.6+4.6=14.2$(Å) (corresponding to $2\theta \fallingdotseq 6.2°$).[24,28] The XRD results of the Cloisite 25 A in Figure 1(a) shows that it has a bilayer structure. Figure 2 shows the XRD patterns of SAN nanocomposites. The XRD pattern of the NEP0 has a peak of the (001) plane at 3.1° and another peak at 5.9°. As the amount of epoxy oligomer used for the nanocomposite preparation is increased, we can see from Figure 2 that the (001) plane peak moves to a lower angle and the peak height diminishes. This suggests that the gallery height and the amount of exfoliation were increased by the compatibilization effect of the epoxy segment. However, the peak at $2\theta=5.9°$ in Figure 2(a) moved to higher

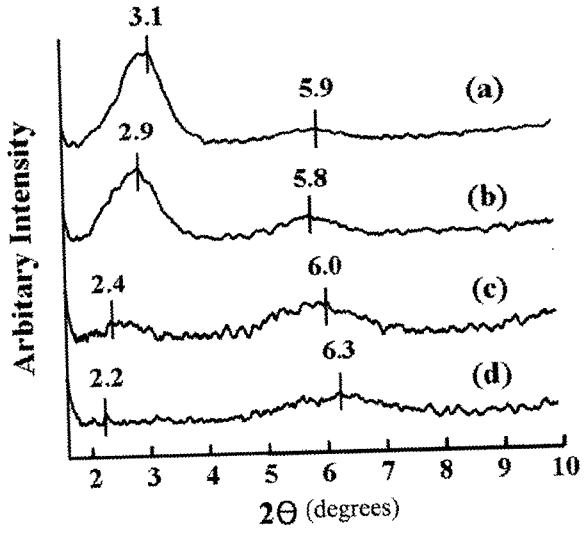


**Figure 2.** XRD patterns of (a) NEP0, (b) NEP1, (c) NEP3, and (d) NEP5.

angle at high levels of epoxy oligomer. These results showed that this peak was not of the (002) plane, because the peak position did not maintain the angle which was two times that of the (001) plane and the relative height of this peak around $2\theta=5.9°$ increased compared to that of the (001) plane as the content of epoxy oligomer was increased.

Similar variations of the XRD patterns were also reported by Ko *et al.* in the nanocomposites of styrenic polymer/organoclay.[29,30] They observed that a peak around $2\theta=6°$ moved to higher angle and its peak height increased as annealing time at 210°C increased[29] or the extrusion cycle increased.[30] They explain the results by postulating that the ammonium cations can escape together with the intercalated polymer to recover the entropy loss due to the nano-confined geometry in the gallery when interaction between ammonium cations and intercalated polymer is high enough to partially compensate for the ionic interaction between the silicate surface and ammonium cation. This diminution of ammonium cations in the gallery induces a change of the alkyl chain arrangement from a bilayer to monolayer structure. They also observed that this extrication is more evident, compared to the PS homopolymer, in the styreic polymers copolymerized with polar monomers such as AN or methylvinyloxazoline, because of enhanced interactions between ammonium cations and polar monomers. Our results may be summarized as follows. During the preparation of the nanocomposite via *in-situ* polymerization two different, competitive processes took place: the intercalation or exfoliation phenomena and the extrication of ammonium cations together with the polymer. Both phenomena were enhanced by an epoxy oligomer, because it could induce inter-gallery polymerization, and it also could increase the interaction between ammonium cations and matrix polymer.

XRD patterns of the PS nanocomposites in Figure 3 showed similar results. However, SEP0 had no peak at the position around $2\theta=6°$. This showed that the extrication of ammonium cations was insignificant in this sample because there was no polar monomer such as AN or an epoxy segment in the matrix polymer, which can interact affirmatively with ammonium cations and can help the extrication of the ammonium cations. Figure 3 also showed, as in Figure 2, a new peak around $2\theta=6°$ that developed and moved to higher angles as the content of the epoxy oligomer was increased, which supports our previous explanation that the epoxy segment enhanced the extrication of ammonium cations, together with the exfoliation of the organoclay.

The alkyl chain rearrangement from a bilayer structure to monolayer structure was also observed in our previous study regarding poly(ethylene-*co*-vinyl alcohol)/Cloisite 25 A nanocomposites prepared by a solution-precipitation method, where the polymer solution containing the organoclay was precipitated with an excess amount of methanol to yield the nanocomposite.[31] This, together with our present results, shows that the extrication of ammonium cations can occu

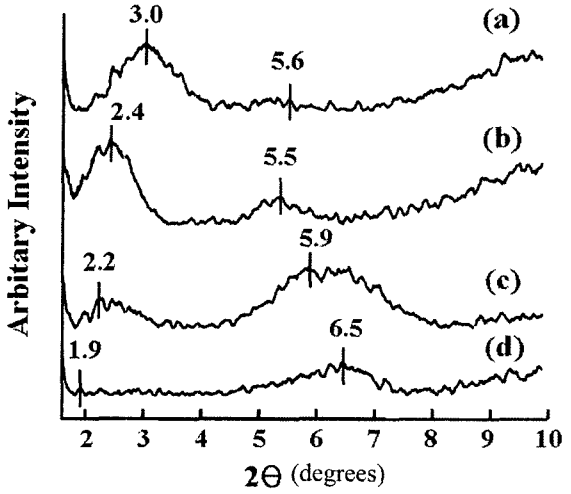


**Figure 3.** XRD patterns of (a) SEP0, (b) SEP1, (c) SEP3, and (d) SEP5.

during polymerization or mixing in solution as well as during compounding or annealing at the melt state.

**TEM.** The TEM micrographs of SAN or PS nanocomposites with organoclay are shown in Figure 4, where the dark lines are the silicate layers in the polymer matrix. The TEM micrograph of NEP0 (Figure 4(a)) showed that the organoclay is dispersed heterogeneously in the micron-scale at the SAN matrix. However, Figure 4(c) and (e) show that this heterogeneity decreases when an azoinitiator linked to an epoxy oligomer was used, where we could see that the thickness of dispersed organoclay was predominantly less than 40 nm. This shows that the delamination of the organoclay was effectively enhanced by the epoxy segment. In TEM micrographs of higher magnification, the morphology of NEP0 (Figure 4(b)) showed a highly parallel alignment of the layers which retained regular spacing, showing that an ordered intercalated structure was dominant in this sample. However, in Figure 4(d) and (f), we could see that this regularity was disturbed. The exfoliated silicate layers were seen together with the regions where dark and light bands alternated with various degrees of swelling. There was also a region, in Figure 4(d) and (f), where the silicate layers lay too close to discern each layer. These morphologies observed by TEM support the XRD results that suggest the epoxy segment induces both phenomena: the delamination or swell-

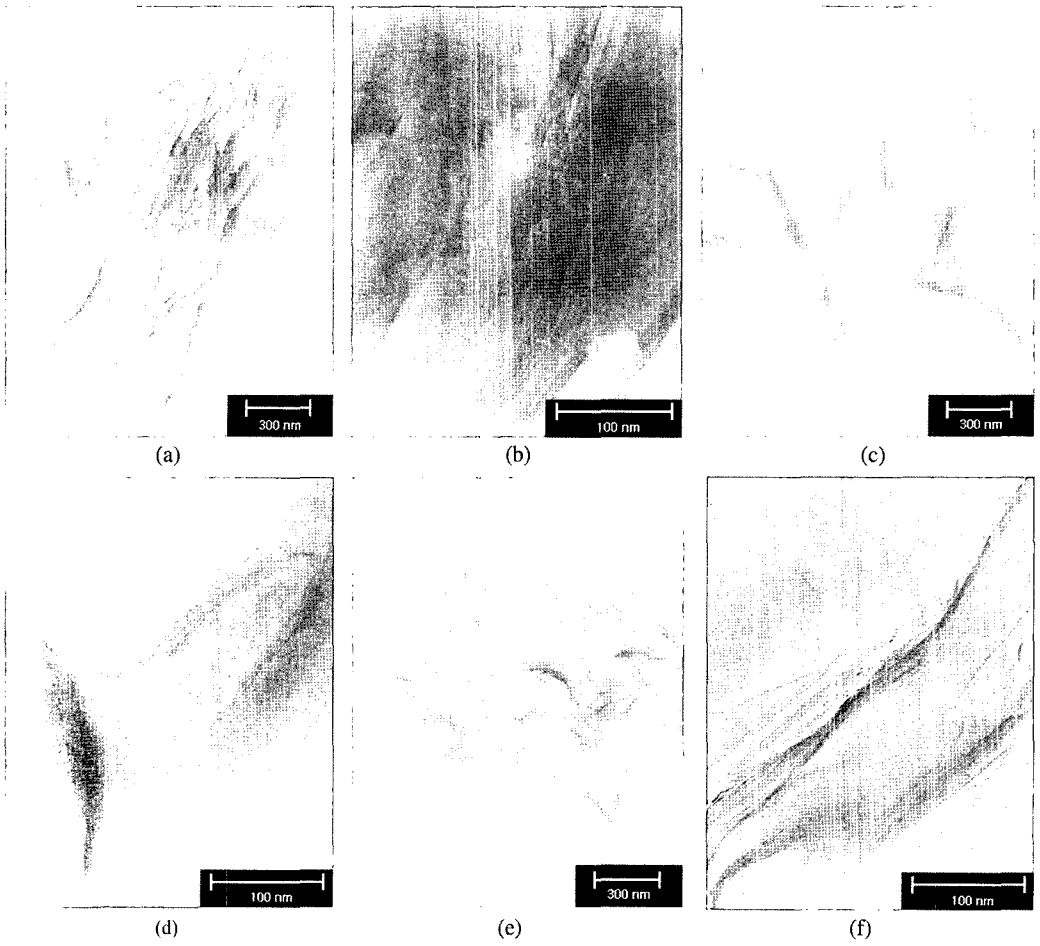


**Figure 4.** TEM micrographs of a styrenic polymer/organoclay nanocompoiste : (a) and (b) NEP0, (c) and (d) NEP5, (e) and (f) SEP5.

ing of the organoclay and a reduction of the gallery height.

**Thermal and Mechanical Properties.** The glass-rubber transition temperatures, $T_g$'s, of styrenic polymer/organoclay nanocomposites measured by DSC are shown in Table II, where we could see that the nanocomposites prepared with ACPC-Epoxy generally had lower $T_g$ values compared with those prepared with AIBN, however the degree of $T_g$ depression was not directly related to the amount of the epoxy segment. In the nanocomposites, the $T_g$ of matrix polymer generally increased compared to the pristine polymer because the segmental motions of the polymer chains were restricted at the organic-inorganic interface. This was likely due to the confinement of the polymer chains between the silicate layers as well as the silicate surface-polymer interaction in the nanostructured composites.[32,33] The enhanced fine dispersion of the organoclay in the polymer matrix in the presence of the epoxy segment can increase the $T_g$ value. However the extrication of ammonium cations together with the intercalated matrix polymer can decrease the $T_g$ value because this induced a reduction of the intercalated polymer chains. The plasticizing effect of the extricated ammonium cation and the epoxy segment can also cause a reduction of the $T_g$ of the matrix polymer. So the results for $T_g$ in Table II suggested that the factors which caused $T_g$ reduction overshadowed the factors which can cause a $T_g$ increase when ACPC-Epoxy was used instead of AIBN, although the results were not simply related to the amount of the epoxy segment.

The tensile storage modulus, $E'$, measured by DMTA is shown in Figure 5 and Figure 6, where it was noted that the glass-rubber transition occurred at lower temperature when the ACPC-Epoxy was used, and as compared to those prepared with AIBN. These results were similar to that of the $T_g$ behavior shown in Table II, and the reasons of this behavior might be the reduction of intercalated polymer, and the plasticizing effect of extricated ammonium cation and epoxy segment, as we explained in $T_g$ behavior before.

The $E'$ values at the glassy region showed mixed results.

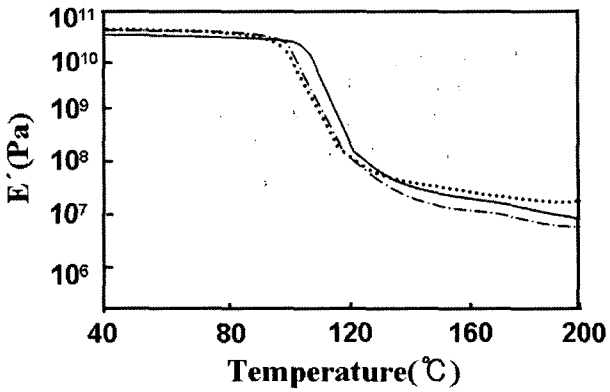


**Figure 5.** Tensile storage modulus of SAN/organoclay nanocomposites: (——) NEP0, (—·—·—) NEP1, (------) NEP5.

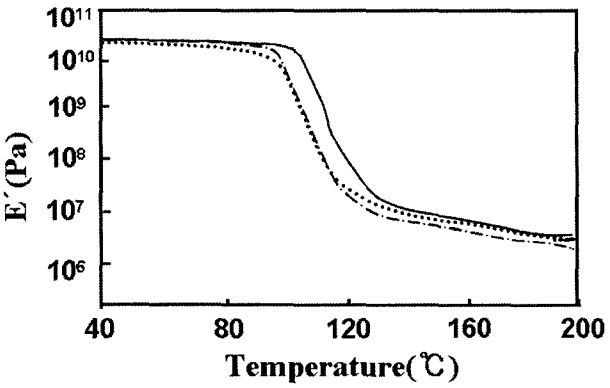


**Figure 6.** Tensile storage modulus of PS/organoclay nanocomposites: (——) SEP0, (—·—·—) SEP1, (------) SEP5.

**Table II. Characteristics of the Styrenic Polymer/Organoclay Nanocomposites**

| Sample | Polymerization Yield (%) | Molecular Weight | | Content of Organoclay[a] (%) | $T_g$ (°C) |
|---|---|---|---|---|---|
| | | $\overline{M}_n$ | $\overline{M}_w$ | | |
| SAN Nanocomposite | | | | | |
| NEP0 | 81 | 61,300 | 195,900 | 5.3 | 110 |
| NEP1 | 80 | 19,400 | 120,000 | 5.4 | 104 |
| NEP3 | 79 | 17,900 | 185,700 | 5.8 | 99 |
| NEP5 | 86 | 22,400 | 438,300 | 5.5 | 101 |
| PS Nanocomposite | | | | | |
| SEP0 | 83 | 74,700 | 209,900 | 4.8 | 105 |
| SEP1 | 86 | 34,200 | 141,900 | 5.2 | 103 |
| SEP3 | 82 | 23,500 | 138,100 | 5.5 | 101 |
| SEP5 | 85 | 40,100 | 941,400 | 5.0 | 102 |

[a]Calculated from the residue after ignition.

A slight enhancement of the $E'$ value in SAN nanocomposites was observed, whereas there was a slight reduction of the $E'$ value in PS nanocomposites, when they were prepared with ACPC-Epoxy instead of AIBN. We anticipated that the enhanced fine dispersion of the organoclay in the polymer matrix could improve $E'$, whereas the reduction of the intercalated polymer chain, the plasticizing effect of extricated ammonium cations and the epoxy segment, could reduce the $E'$ value. These results of the $E'$ values at the glassy region in Figure 5 and Figure 6 were due to the complicated contribution of these factors caused by the epoxy segment.

## Conclusions

Our experimental results showed that the epoxy segment linked to an azoinitiator enhanced both the delamination of the organoclay and the extrication of ammonium cations into the polymer matrix during the polymerization of styrenic polymers in the presence of organoclay. The decreased glass-rubber transition temperature showed that the effect of the extrication of ammonium cations was predominant in this behavior. More complicated results for the $E'$ value showed that organoclay delamination and ammonium cation extrication competitively influenced $E'$ variations. The XRD results showed that the diminution of ammonium cations in the gallery by extrication could induce a change in the alkyl chain structure from a bilayer to monolayer structure.

**Acknowledgements.** This work was supported by University of Ulsan Research Fund of 2005.

## References

(1) P. C. Le Baron, Z. Wang, and T. J. Pinnavaia, *Appl. Clay Sci.*, **15**, 11 (1999).
(2) E. P. Giannelis, *Appl.Organometal. Chem.*, **12**, 675 (1998).
(3) T. J. Pinnavaia and G. W. Beall, Eds., *Polymer-Clay Nanocomposites*, John Wiley & Sons, New York, 2000.
(4) L. A. Utracki, *Clay-Containing Polymeric Nanocomposites*, Rapra Technology Limited, Shawbury, 2004.
(5) H. Acharya and S. K. Srivastava, *Macromol. Res.*, **14**, 132 (2006).
(6) S.-Y. Park and Y.-H. Cho, *Macromol. Res.*, **13**, 156 (2005).
(7) J.-Y. Kim, S.-H. Hwang, Y. S. Hong, W. Huh, and S.-W. Lee, *Polymer (Korea)*, **29**, 87 (2005).
(8) S.-U. Lee, I.-H. Oh, J. H. Lee, K.-Y. Choi, and S.-G. Lee, *Polymer (Korea)*, **29**, 271 (2005).
(9) C. Zeng and L. J. Lee, *Macromolecules*, **34**, 4098 (2001).
(10) A. B. Morgan and J. W. Gilman, *J. Appl. Polym. Sci.*, **87**, 1329 (2003).
(11) Y. S. Choi, M. H. Choi, K. H. Wang, S. O. Kim, Y. K. Kim, and I. J. Chung, *Macromolecules*, **34**, 8978 (2001).
(12) M. W. Weimer, H. Chen, E. P. Giannelis, and D. Y. Sogah, *J. Am. Chem. Soc.*, **121**, 1615 (1999).
(13) E. Manias, A. Touny, L. Wu, K. Strawhecker, B. Lu, and T. C. Chung, *Chem. Mater.*, **13**, 3516 (2001).
(14) P. Aranda and E. Ruiz-Hitzky, *Chem. Mater.*, **4**, 1395 (1992).
(15) J. Wu and M. M. Lerner, *Chem. Mater.*, **5**, 835 (1993).
(16) H. R. Fischer, L. H. Gielgens, and T. P. M. Koster, *Acta Polym.*, **50**, 122 (1999).
(17) B. Liao, M. Song, H. Liang, and Y. Pang, *Polymer*, **42**, 10007 (2001).
(18) H. M. Jeong and Y. T. Ahn, *Macromol. Res.*, **13**, 102 (2005).
(19) H. M. Jeong, M. Y. Choi, and Y. T. Ahn, *Macromol. Res.*, **14**, 312 (2006).
(20) H. M. Jeong, J. S. Choi, Y. T. Ahn, and K. H. Kwon, *J. Appl. Polym. Sci.*, **99**, 2841 (2006).
(21) M. Kawasumi, N. Hasegawa, M. Kato, A. Usuki, and A. Okada, *Macromolecules*, **30**, 6333 (1997).
(22) M. Kato, A. Usuki, and A. Okada, *J. Appl. Polym. Sci.*, **66**, 1781 (1997).
(23) A. Usuki, M. Kato, A. Okada, and T. Kurauchi, *J. Appl. Polym. Sci.*, **63**, 137 (1997).
(24) H. Ishida, S. Campbell, and J. Blackwell, *Chem. Mater.*, **12**, 1260 (2000).
(25) T. O. Ahn, J. H. Kim, J. C. Lee, H. M. Jeong, and J.-Y. Park, *J. Polym. Sci., Polym. Chem.*, **31**, 435 (1993).
(26) R. A. Vaia, R. K. Teukolsky, and E. P. Giannelis, *Chem. Mater.*, **6**, 1017 (1994).
(27) G. Lagaly, *Solid State Ionics*, **22**, 43 (1986).
(28) M. B. Ko, M. Park, J. Kim, and C. R. Choe, *Kor. Polym. J.*, **8**, 95 (2000).
(29) J. T. Yoon, W. H. Jo, M. S. Lee, and M. B. Ko, *Polymer*, **42**, 329 (2001).
(30) M. B. Ko, J. Kim, and C. R. Choe, *Korea Polym. J.*, **8**, 120 (2000).
(31) H. M. Jeong, B. C. Kim, E. H. Kim, *J. Mater. Sci.*, **40**, 3783 (2005).
(32) P. Uthirakumar, K. S. Nahm, Y. B. Hahn, and Y.-S. Lee, *Eur. Polym. J.*, **40**, 2437 (2004).
(33) M. W. Noh and D. C. Lee, *Polym. Bull.*, **42**, 619 (1999).